

---

**MAJOR PAPER**

---

## **Factors that Differentiate between Endometriosis-associated Ovarian Cancer and Benign Ovarian Endometriosis with Mural Nodules**

Yasuhito Tanase<sup>1</sup>, Ryuji Kawaguchi<sup>1</sup>, Junko Takahama<sup>2</sup>, and Hiroshi Kobayashi<sup>1\*</sup>

**Purpose:** Mural nodules and papillary projections can be seen in benign ovarian endometriosis (OE) and malignant transformation of OE (endometriosis-associated ovarian cancer [EAOC]), which can pose a challenging diagnostic dilemma to clinicians. We identify the preoperative imaging characteristics helpful to the differential diagnosis between benign OE with mural nodules and EAOC.

**Materials and Methods:** This was a retrospective study of 82 patients who were diagnosed pathologically to have OE with mural nodules ( $n = 42$ ) and malignant transformations of these tumors ( $n = 40$ ) at the Nara Medical University Hospital from January 2008 to January 2015. All patients were assessed with contrast-enhanced magnetic resonance imaging (MRI) before surgery. Patient demographics, and clinical and pathologic features were analyzed to detect the significant differences between the two groups.

**Results:** Histological examinations of resected OE tissue specimens revealed that a majority (78.6%) of the mural nodular lesions were retracted blood clots. We found that the patients with malignant mural nodules, when compared to those with benign nodules, were older, had larger cyst diameters and larger mural nodule sizes, and were more likely to exhibit a taller than wider lesion. They were also more likely to present with various signal intensities on  $T_1$ -weighted images ( $T_1$ WI), high-signal intensity on  $T_2$ -weighted images ( $T_2$ WI), a lower proportion of shading on  $T_2$ WI, and were more likely to show an anterior location of the cyst. In the multivariate logistic regression analysis, “Height” ( $>1.5$  cm) and “Height-Width ratio (HWR)” ( $>0.9$ ) of mural nodules, maximum diameter of the cyst ( $>7.9$  cm), and age at diagnosis ( $>43$  years) were independent predictors to distinguish EAOC from OE with mural nodules.

**Conclusion:** The “Height” and “HWR” of the mural nodules in the cyst may yield a novel potential diagnostic factor for differentiating EAOC from benign OE with mural nodules.

**Keywords:** *endometriosis, epithelial ovarian cancer, mural nodules, ultrasonography, diagnosis*

### **Introduction**

Endometriosis affects 5–10% of the female population in the reproductive age group.<sup>1</sup> Endometriosis may be associated with increased risk of ovarian cancer.<sup>2,3</sup> In general practice, transvaginal ultrasonography is the first line imaging examination to search for adnexal masses, including ovarian endometriosis (OE).<sup>4–9</sup> Ultrasonography is a useful technique for the diagnosis of benign adnexal masses. Ultrasonographic appearances of OE include a unilocular cyst with ground glass pattern

or homogeneous low-level echogenicity without solid parts, papillary formations, or mural nodules. Typical OE may be easier to discriminate from other adnexal masses.<sup>9</sup> However, the ultrasound morphology of OE is variable, possibly due to the appearances of solid components, mural nodules, or papillary projections from a cyst wall and the degradation of internal blood products or retracted blood clots that appeared solid over time.<sup>10</sup> A blood clot next to the inner wall of the cyst containing the ground glass background shows an oval- or crescent-shaped lesion.<sup>11</sup> In general, the presence of mural nodules and papillary projections is considered to constitute evidence of malignancy.<sup>12</sup> Therefore, these sonographic appearances were the most common forms mimicking malignancy.

Magnetic resonance (MR) imaging is the recommended imaging modality of choice for the preoperative workup of OE and complex cases of OE with extensive adhesion formation.<sup>7</sup> Clinicians also use pelvic MR imaging in some cases with nontypical morphologic changes and ultrasonographic

---

<sup>1</sup>Department of Obstetrics and Gynecology, Nara Medical University, 840 Shijo-cho, Kashihara, Nara 634-8522, Japan

<sup>2</sup>Department of Radiology, Nara Medical University, Nara, Japan

\*Corresponding author, E-mail: hirokoba@naramed-u.ac.jp

©2017 Japanese Society for Magnetic Resonance in Medicine

This work is licensed under a Creative Commons Attribution-NonCommercial-NoDerivatives International License.

Received: July 26, 2016 | Accepted: July 5, 2017

findings similar to endometriosis-associated ovarian cancer (EAOC) to differentiate malignant adnexal masses from OE.<sup>8</sup> MRI findings of various degrees of solid portions, mural nodules, papillary projections, thick septations, or strong vascularization are strongly suggestive of ovarian malignancy.<sup>3,7,12–14</sup> The gadolinium-based contrast medium was used primarily to improve detection and characterization of ovarian lesions; its introduction has improved diagnostic accuracy in OE patients with suspected malignancy. Furthermore, such imaging modalities as diffusion-weighted (DWI) and dynamic contrast-enhanced imaging can be of additional value in the diagnosis of EAOC.<sup>14</sup> Although several studies have described MR imaging features of complex cases of OE, they rarely focused on imaging findings that included the shape and location of a mural nodule or papillary projection of a cystic ovarian lesion. To our knowledge, few studies have evaluated the characteristics of MR imaging with respect to benign mural nodular components, mimicking malignant transformation.

We evaluated the role of MR findings focused on the morphological features in discriminating between EAOC and benign OE with mural nodular components.

## Materials and Methods

The study was approved by the ethics committee of Nara Medical University and written informed consent was obtained from all patients. This was a retrospective data collection of 82 cases operated upon at the Department of Obstetrics and Gynecology, Nara Medical University between January 2008 and January 2015, for a pathologically confirmed benign OE with mural nodular components (OE group,  $n = 42$ ) and malignant transformations of these tumors (EAOC group,  $n = 40$ ). In our hospital, routine evaluation of adnexal masses always includes tumor marker detection, including CA125 and imaging studies, such as ultrasonography and MR imaging. Ultrasonographic evaluations were performed using the sonographic instrument (ESAOTE-HITACHI Logos; Genoa, Italy). MR imaging was obtained on a 3Tesla system (Magnetom Verio; Siemens Healthcare, Erlangen, Germany) with 32-element body array coil. The protocol of our routine MR examination was as follows: T<sub>2</sub>-weighted images (T<sub>2</sub>WI; sagittal; turbo spin-echo [TSE], repetition time [TR]/echo time [TE] = 4000/89, Matrix = 512/307, field of view [FOV] = 200 × 200, echo train length [ETL] = 19, slice thickness = 3 mm), T<sub>1</sub>-weighted images (T<sub>1</sub>WI; axial; spin-echo [SE], TR/TE = 450/12, Matrix = 320/192, FOV = 200 × 200, slice thickness = 3 mm), T<sub>2</sub>WI (axial; SPACE, TR/TE = 2700/287, Matrix = 256/256, FOV = 250 × 250, slice thickness = 1.0 mm, flip angle mode = T<sub>2</sub> var), and HASTE (coronal; TR/TE = 2000/88, Matrix = 320/240, FOV = 280 × 280, slice thickness = 5 mm). All cases underwent dynamic contrast-enhanced MRI with a dose of 10 ml of meglumine gadopentetate (Magnevist; Bayer, Leverkusen, Germany), which was injected with an automated injector at a rate of 2 mL/sec and

followed by a 20 mL saline flush. Dynamic MRI was performed at three continuous fat-saturated T<sub>1</sub>WI (axial; volumetric interpolated breath-hold examination [VIBE]: TR/TE = 3.74/1.38, FA = 11, Matrix = 256/256, FOV = 250 × 200, slice thickness = 1.0 mm) in 60, 120, and 180 seconds after injection. These diagnostic imaging modalities are acceptable for excluding the possibility of malignancy before surgery and choosing appropriate treatment options.

During the study, 180 patients underwent surgery for OE. Among these patients, 42 with mural nodular components mimicking malignant tumors by ultrasonography were pathologically confirmed to have benign OE. A total of 138 patients with benign OE without mural nodular components were originally excluded from the study, and 50 patients with EAOC were pathologically confirmed to have a malignancy. International Federation of Gynecology and Obstetrics (FIGO) stage and the final pathological diagnosis were confirmed. The EAOC tumors contained a mixture of solid, cystic, and nodular patterns in various proportions; cystic masses with mural nodules in 40 (80%) and solid masses or almost solid masses with small cystic parts in 10 (20%). When measuring the diameter of a cyst and a mural nodule we excluded the 10 cases with solid masses. The remaining 40 cases fulfilled Sampson and Scott criteria.<sup>15</sup>

Baseline and histologic characteristics were assessed for the two groups separately and concurrently with the following variables: age at diagnosis, nulliparity, menopausal status, preoperative value of CA125, and the MR imaging characteristics. The preoperative MR characteristics of the two groups were analyzed: signal intensity on T<sub>1</sub>WI and T<sub>2</sub>WI, presence of shading and enhancement pattern, the largest diameter of each adnexal mass, the size of a mural nodular component, location of a mural nodule, and other characteristics of a mural nodule, respectively. The signal intensity of the cystic parts was analyzed on T<sub>1</sub>WI and T<sub>2</sub>WI as low, intermediate, or high relative to that of striated muscle. We defined the size of a mural nodule according to “Height” and “Width.” The term “Height” indicated maximum vertical length from the bottom of the cyst to the top of the nodule. The term “Width” indicated maximum perpendicular length to the “Height” (Fig. 1). For each case, the largest dimensions of mural nodules were used to determine “Height” and “Width.” Mural nodular “Height-Width” ratio (HWR) also was calculated. In cases with multiple nodules the maximum lesion was measured. We evaluated the location of a mural nodule using a four-quadrant identification system, representing the anterior upper quadrant (AUQ), anterior lower quadrant (ALQ), posterior upper quadrant (PUQ), and posterior lower quadrant (PLQ; Fig. 2).

Clinical information was gathered from the electronic medical records and pathologic examination notes. MRI findings were reviewed retrospectively by one gynecologic oncologist (Y.T.) and one radiologist (J.T.) who reached consensus agreement after discussing the findings. All pathological sections were analyzed by a highly qualified pathologist.

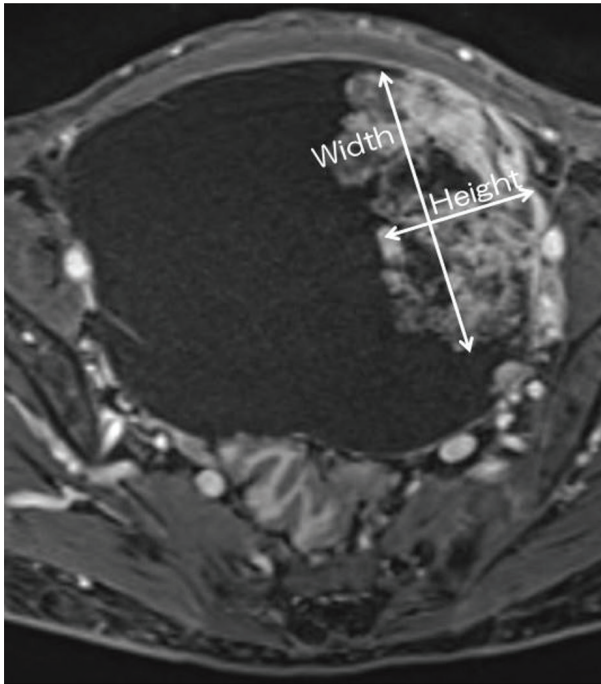


**Fig 1.** The Height-Width ratio. Clear cell carcinoma of the ovary, 56 years old, Federation of Gynecology and Obstetrics (FIGO) Stage IC1. Axial postcontrast T<sub>1</sub>-weighted images (T<sub>1</sub>WI) shows hyperintense mural nodules. The term “Height” indicates maximum vertical length from the bottom of the cyst to the top of the nodule. The term “Width” indicates maximum perpendicular length to the “Height.”

### Statistical analysis

The clinical characteristics for the two groups were compared using the Student *t*-test,  $\chi^2$  test, or Fisher’s exact test for univariate analyses. Multivariate logistic regression analysis of 82 cases was performed to assess independent predictors that allowed the differential diagnosis of the two groups. Significant variables by univariate analyses underwent further multivariate analyses. On multivariate analysis, the location of a mural nodule was divided into two subgroups: AUQ plus ALQ (anterior group) versus PUQ plus PLQ (posterior group). With respect to the signal intensity of cystic parts on T<sub>1</sub>WI and T<sub>2</sub>WI, we divided the patients into two subgroups: patients with the low and intermediate signal intensity versus those with the high-signal intensity.

A receiver-operating characteristic (ROC) curve analysis was calculated using significant predictors (as determined via multivariate regression) to determine the areas under the curve (AUCs), derive best suitable cutoff values of each parameter, and assess model discrimination and predictive accuracy, including sensitivity, specificity, and positive and negative predictive values (PPV and NPV). The optimal cutoff point was determined by ROC curve based on the Youden index. Analyses were performed using commercially available software packages (SPSS Statistics for Windows version 17.0; IBM Corp., NY, USA and Medcalc for Windows version 11.4.2.0; Medcalc, Ostend, Belgium). Values of  $P < 0.05$  were deemed to indicate statistical significance.

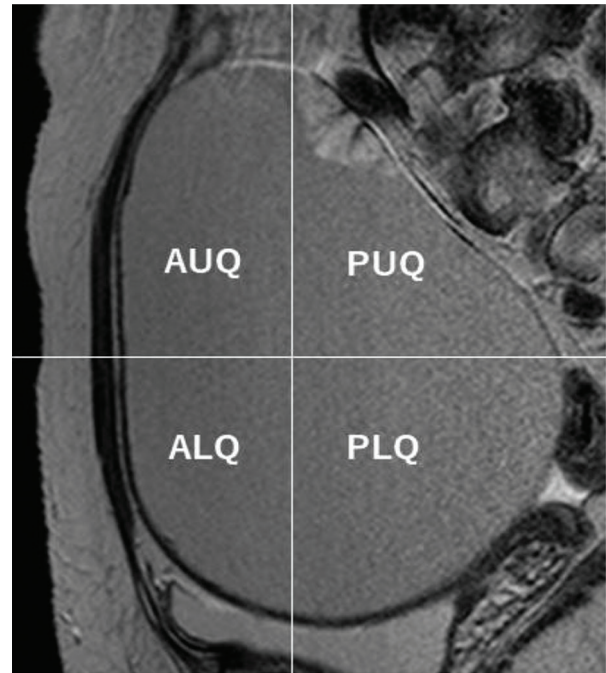


**Fig 2.** The location of a mural nodule using a four-quadrant identification system. ALQ, anterior lower quadrant; AUQ, anterior upper quadrant; PLQ, posterior lower quadrant; PUQ, posterior upper quadrant.

### Results

The study population consisted of 42 benign OE group patients with mural nodules (mean age,  $39 \pm 10$ ) and 40 EAOC patients (mean age,  $54 \pm 9$ ). The characteristics of the 82 patients are summarized in Table 1. The majority ( $n = 33$ , 78.6%) of these benign mural nodules are blood clots. Our study showed MR imaging features more typical of malignant (Fig. 3) and benign (Fig. 4) lesions.

As presented in Table 1, the results of the univariate analysis indicated that the patient age ( $P < 0.001$ ); premenopausal status ( $P < 0.001$ ); maximum diameter of the cyst ( $P < 0.001$ ); the “Height,” “Width,” and “HWR” of mural nodules ( $P < 0.001$ ); location of the lesion within the cyst ( $P < 0.001$ ); proportion of shading ( $P < 0.01$ ); and an imaging pattern of the cystic lesions were significantly associated with malignancy. With regard to the location of a mural nodule, the OE group had nodules located mainly on the PLQ (71.4%) and PUQ (19.0%) of the cyst. In the majority of OE cases (90.4%), the nodular lesions were located on the posterior wall of the cyst. In contrast, the mural nodules in the EAOC group were located on the ALQ (40.0%) and AUQ (22.5%) of the cyst. Mural nodules within EAOC tumors were more likely to show an anterior location compared to benign OE cysts (62.5% vs. 9.6%,  $P < 0.001$ ).

Even in the OE group, nine (21.4%) of 42 patients had enhancing mural nodules, whose pathologies were atypical endometriosis ( $n = 3$ ), adenofibroma ( $n = 2$ ), fibrothecoma ( $n = 2$ ), and papillary proliferation of epithelium ( $n = 2$ ).

**Table 1.** Baseline characteristics of two groups

Patient and clinical characteristics	OE with benign mural nodules	EAOc	P value
Number	42	40	
Pathology	Blood clot ( <i>n</i> = 3) Atypical feature ( <i>n</i> = 3) Adenofibroma ( <i>n</i> = 2) Fibrothecoma ( <i>n</i> = 2) Papillary proliferation ( <i>n</i> = 2)	Clear cell carcinoma ( <i>n</i> = 22), Endometrioid carcinoma ( <i>n</i> = 11) Serous carcinoma ( <i>n</i> = 3), Mucinous carcinoma ( <i>n</i> = 2), Undifferentiated carcinoma ( <i>n</i> = 1), Transitional carcinoma ( <i>n</i> = 1)	
FIGO stage	–	I ( <i>n</i> = 35), II ( <i>n</i> = 0), III ( <i>n</i> = 3), IV ( <i>n</i> = 2)	
Age at diagnosis, mean ± SD	39.1 ± 10.3	54.3 ± 8.9	<0.001
Median (range)	39 (26 – 68)	52 (39 – 75)	
Nulliparous <i>n</i> (%)	21 (50%)	16 (40%)	0.55
Premenopause <i>n</i> (%)	38 (90.5%)	14 (35%)	<0.001
CA125 (IU/l)			
Mean ± SD	86.8 ± 99.4	992.5 ± 3166	0.07
Median (range)	34.5 (6 – 437)	60.5 (7 – 15451)	
The size of a cyst (cm)*			
Mean ± SD	6.6 ± 3.2	10.9 ± 3.9	<0.001
Median (range)	5.9 (2.5 – 19.1)	10.4 (2.9 – 19)	
Height (cm), mean ± SD	0.7 ± 0.3	3.7 ± 2.3	<0.001
Median (range)	0.7 (0.2 – 1.6)	3.3 (1 – 10.8)	
Width (cm), mean ± SD	1.5 ± 1.0	3.5 ± 2.3	<0.001
Median (range)	1.2 (0.5 – 4.9)	2.9 (0.9 – 10.6)	
HWR of mural nodule,			
Mean ± SD	0.5 ± 0.2	1.1 ± 0.2	<0.001
Median (range)	0.56 (0.20 – 0.68)	1.09 (0.47 – 1.63)	
Location (%)			
AUQ	2 (4.8%)	9 (22.5%)	<0.001
ALQ	2 (4.8%)	16 (40%)	
PUQ	8 (19%)	3 (7.5%)	
PLQ	30 (71.4%)	12 (30%)	
Signal intensity of cystic part			
On T <sub>1</sub> WI			
Low	0 (0%)	13 (32.5%)	<0.001
Intermediate	4 (9.5%)	13 (32.5%)	
High	38 (90.5%)	14 (35%)	
On T <sub>2</sub> WI			
Low	3 (7.1%)	0 (0%)	0.009
Intermediate	13 (31%)	3 (7.5%)	
High	26 (61.9%)	37 (92.5%)	
Shading			
<i>n</i> (%)	27 (64.3%)	7 (14%)	<0.01

\*Maximum diameter of the cyst. ALQ, anterior lower quadrant; AUQ, anterior upper quadrant; FIGO, Federation of Gynecology and Obstetrics; PLQ, posterior lower quadrant; PUQ, posterior upper quadrant; SD, standard deviation; T<sub>1</sub>WI, T<sub>1</sub>weighted image; T<sub>2</sub>WI, T<sub>2</sub>weighted image.

Endometrial cysts with benign mural nodules rarely showed low-signal intensity on T<sub>1</sub>WI and various signal intensities on T<sub>2</sub>WI. Endometrial cysts with malignant transformation rarely showed low-signal intensity on T<sub>2</sub>WI and usually had enhanced mural nodules. Moreover, shading on T<sub>2</sub>WI was observed in 27 (64.3%) and 7 (14%) cases in the OE and EAOc groups, respectively.

All variables showing significant values in the univariate analysis (age at diagnosis, size of a cyst, “Height,” “HWR,” location of mural nodules, the proportion of shading, and signal intensity on T<sub>1</sub>WI and T<sub>2</sub>WI of the cystic lesions) that were statistically significant in the correlation analysis were included in the multivariate analysis. The parameter “Width” was excluded due to a strong correlation between “Height”

and “Width” (Spearman rank correlation coefficient was 0.85). The parameter “Premenopausal status” also was excluded due to a strong correlation between “Age” and “Premenopausal status” (Spearman rank correlation coefficient was 0.91). In multivariate analysis for the associations of EAO, “Height,” “HWR,” a maximum diameter of the cyst, and age at diagnosis resulted in the best the discrimination of patients with malignant or benign mural nodules (Table 2).

ROC curves showed that AUC, 95% confidence interval (CI), optimum diagnostic cutoff value, sensitivity, specificity, PPV, and NPV predicted EAO (Table 3). “Height” was the most valuable predictor (AUC, 0.99; 95% CI, 0.97–1.0;  $P < 0.01$ ). The best cutoff value associated with “Height” was 1.5 cm. The sensitivity and specificity of this test using the cutoff value of 1.5 were 95% and 95.2%, respectively. The positive and negative predictive values were 95% and 95.2%, respectively. Other tests, including “HWR,” a maximum diameter of the cyst, and age at diagnosis, showed statistically significant results.

## Discussion

Distinguishing the EAO group from the OE group is an urgent issue. An ultrasonographic finding, such as existing mural nodules, affected as many as 42 (23.3%) of 180 women with pathologically-proven benign OE. A blood clot was diagnosed in the majority of cases (33 cases, 78.6%), while in the remaining 9 (21.4%) cases, various other benign lesions with contrast enhancement of the mural nodules were diagnosed. Awareness of such lesions and interpretation of imaging studies in the OE group requires a critical review to detect malignant tumors. We evaluated 42 benign OE cases with mural nodules (OE group) and 40 malignant EAO cases (EAO group).

Firstly, the univariate analysis showed that age at diagnosis, maximum diameter of the cyst, size, and shape (“Height,” “Width,” and “HWR”), location of mural nodules, premenopausal status, and proportion of shading and signal intensity on T<sub>1</sub>WI and T<sub>2</sub>WI of the cystic lesions were significantly different between the two groups; these parameters

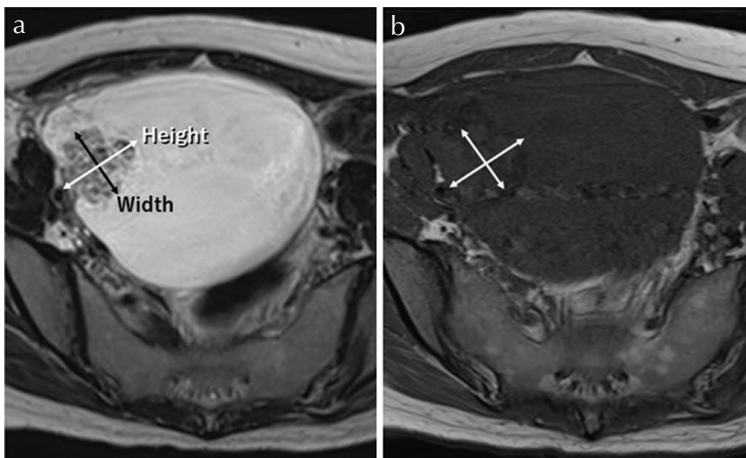


**Fig 3.** Mural nodules with malignant features on magnetic resonance (MR) imaging. Clear cell carcinoma, stage I C3, in 39-year-old woman. (a) On axial T<sub>2</sub>-weighted images (T<sub>2</sub>WI), the mass demonstrates high-signal intensity with a mural nodule on the anterior-right sided wall of the cyst. (b) The signal intensity of the mass on axial T<sub>1</sub>-weighted images (T<sub>1</sub>WI) indicated homogenous low signal. “Height” was 2.9 cm and “Width” was 2.5 cm. “Height-Width ratio (HWR)” indicated 1.16.

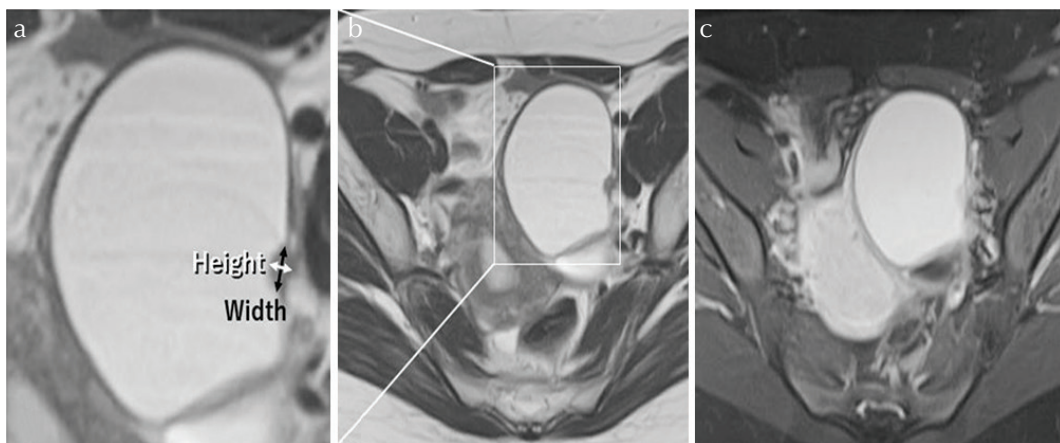


**Fig 4.** Mural nodules with benign features on magnetic resonance (MR) imaging. Endometriotic cyst in 31 years old woman. (a, b) On axial T<sub>2</sub>-weighted images (T<sub>2</sub>WI), left sided mass demonstrates high-signal intensity with mural nodule on the posterior wall of the cyst. (a) A high magnification image of (b), inset. (c) Gadolinium enhanced fat-suppressed T<sub>1</sub>-weighted images (T<sub>1</sub>WI) demonstrates enhancement of the mural nodules. “Height” was 0.4 cm and “Width” was 0.6 cm. “Height-Width ratio (HWR)” indicated 0.67.

**Table 2.** Multivariate logistic regression analysis for the prediction of endometriosis-associated ovarian cancer (EAOC)

Variable	$\beta$	Standard error	Wald	OR (95% CI)	P Value
Age at diagnosis	3.01	1.38	4.77	20.2 (1.4 – 299.6)	0.029
Maximum diameter of the cyst	4.71	1.60	8.65	111.1 (4.8 – 2565.2)	0.003
Height	5.94	1.025	33.56	380 (50.9 – 2835)	<0.0001
HWR	5.91	1.14	26.83	369 (39.4 – 3454.3)	<0.0001
Signal intensity on T <sub>1</sub> WI	-0.671	1.13	0.35	0.5 (0.056 – 4.7)	0.554
Signal intensity on T <sub>2</sub> WI	2.28	1.29	3.11	9.8 (0.8 – 83.8)	0.078
Location	2.16	1.16	3.51	8.7 (0.9 – 83.8)	0.061
Shading	0.47	1.28	0.137	1.6 (0.13 – 19.7)	0.712

CI, confidence interval; HWR, Height-Width ratio; OR, Odds ratio; T<sub>1</sub>WI, T<sub>1</sub>weighted image; T<sub>2</sub>WI, T<sub>2</sub>weighted image.

**Table 3.** The discriminative value of each parameter

Variables	AUC	95% CI	P values	Cutoff value	Sensitivity	Specificity	PPV	NPV
Height	0.99	0.97 – 1.0	<0.01	1.5 (cm)	95	95.2	95	95.2
HWR	0.97	0.94 – 1.0	<0.01	0.9	90	100	100	91.2
Cyst size	0.81	0.71 – 0.91	<0.01	7.9 (cm)	82.5	83.3	82.5	83.3
Age	0.88	0.81 – 0.96	<0.01	43 (y)	92.5	76.2	78.7	91.4

AUC, area under the curve; CI, confidence interval; HWR, Height-Width ratio; PPV, positive predictive values; NPV, negative predictive values.

can help to differentiate between EAOC and benign OE with mural nodules (Table 1). The results of multivariate logistic regression analysis (Table 2) showed that the “Height,” “HWR,” maximum diameter of the cyst, and age at diagnosis were independent factors that can allow differentiation between the EAOC and OE groups. The “Height” and “HWR” may be considered as the most important imaging characteristics of malignant features. Compared to the OE group, the mural nodules of the EAOC group were larger and rather taller than wide. In benign OE with blood clots, ultrasonography might show a hyperechogenic round or crescent-shaped focus that corresponds to a blood clot next to the inner wall of the cyst. These potential factors may influence an important clinical decision, such as the decision to undergo MR imaging and then surgery.

Secondly, so far there was a lack of consensus regarding the exact location of the mural nodular components within the cyst. On univariate analysis, we found that mural nodules located on the abdominal side have a possibility of malignancy. Although an adequate explanation for this asymmetric occurrence of mural nodules within OE has never been established to our knowledge, one possibility is that blood clots that formed easily precipitated to the bottom of the cyst.

Finally, our results confirmed the previous study indicating that: 1) in patients with EAOC, clear cell carcinoma and endometrioid carcinoma were reported most commonly when the primary site was the ovary, 2) approximately 80% of EAOC cases presented with stages I and II disease, and 3) EAOC usually occurs in women aged >40 years old, with a wide age of onset, and present as a large mass (>9 cm).<sup>16</sup> Our data based on

the intensity pattern on T<sub>1</sub>WI and T<sub>2</sub>WI were supported by the previous study.<sup>7</sup> Endometrial cysts have been reported to be hyperintense on T<sub>1</sub>WI and have an intermediate high-signal intensity on T<sub>2</sub>WI.<sup>17,18</sup> Shading was the prevalent pattern in the OE group. This intensity pattern is thought to be caused by a magnetic susceptibility effect generated by hemosiderin in old hemorrhage, densely concentrated fluid, or fibrosis.<sup>19</sup> Once malignant transformation occurs, the intensity pattern on T<sub>1</sub>WI and T<sub>2</sub>WI can change. Endometrial cysts with malignant transformation rarely show low-signal intensity on T<sub>2</sub>WI and usually have enhanced mural nodules.<sup>17,18</sup>

This study has several limitations. Firstly, the mural nodules of the OE group were essentially small, and measurement error became large inevitably. Secondly, it was a retrospective study, and, therefore, there may have been some selection bias. Furthermore, we have mainly focused on imaging findings, including the shape and location of a mural nodule or papillary projection of a cystic ovarian lesion. In the present study, therefore, we did not include DWI and chemical shift images. DWI and apparent diffusion coefficient (ADC) values are sensitive and specific methods for differentiating benign from malignant adnexal masses. Image artifacts due to changes in chemical shift may be more noticeable to predict coagulation.

In conclusion, we studied which features in MR imaging scans could best discriminate between EAOC and benign OE with mural nodular components. First, the EAOC group showed larger mural nodules and was more likely to exhibit taller than wide mural nodules, suggesting that this shape is specific for differentiating malignant from benign nodules. Second, mural

nodules located on the abdominal side may be useful in proper decision-making regarding the diagnosis of malignant transformation. These potential features may help clinicians in the diagnosis. Further clinical study will evaluate the reliability and validity of ultrasound imaging on the shape and location of mural nodules with their corresponding MRI measurements.

## Conflicts of Interest

The authors declare that the research was conducted in the absence of any commercial or financial relationships that could be construed as a potential conflict of interest.

## Acknowledgments

The present study was supported by grant-in-aid for Scientific Research from the Ministry of Education, Science, and Culture of Japan to the Department of Obstetrics and Gynecology, Nara Medical University (to H.K.).

## References

1. D'Hooghe TM, Debrock S, Hill JA, Meuleman C. Endometriosis and subfertility: is the relationship resolved? *Semin Reprod Med* 2003; 21:243–254.
2. Munksgaard PS, Blaakaer J. The association between endometriosis and gynecological cancers and breast cancer: a review of epidemiological data. *Gynecol Oncol* 2011; 123:157–163.
3. Krawczyk N, Banys-Paluchowski M, Schmidt D, Ulrich U, Fehm T. Endometriosis-associated Malignancy. *Geburtshilfe Frauenheilkd* 2016; 76:176–181.
4. Van Holsbeke C, Van Calster B, Guerriero S, et al. Endometriomas: their ultrasound characteristics. *Ultrasound Obstet Gynecol* 2010; 35:730–740.
5. Asch E, Levine D. Variations in appearance of endometriomas. *J Ultrasound Med* 2007; 26:993–1002.
6. Alcázar JL, León M, Galván R, Guerriero S. Assessment of cyst content using mean gray value for discriminating endometrioma from other unilocular cysts in premenopausal women. *Ultrasound Obstet Gynecol* 2010; 35:228–232.
7. Tanaka YO, Yoshizako T, Nishida M, Yamaguchi M, Sugimura K, Itai Y. Ovarian carcinoma in patients with endometriosis: MR imaging findings. *AJR Am J Roentgenol* 2000; 175:1423–1430.
8. Holland TK, Cutner A, Saridogan E, Mavrelou D, Pateman K, Jurkovic D. Ultrasound mapping of pelvic endometriosis: does the location and number of lesions affect the diagnostic accuracy? A multicentre diagnostic accuracy study. *BMC Womens Health* 2013; 13:43.
9. Fraser MA, Agarwal S, Chen I, Singh SS. Routine vs. expert-guided transvaginal ultrasound in the diagnosis of endometriosis: a retrospective review. *Abdom Imaging* 2015; 40:587–594.
10. Saeng-Anan U, Pantasri T, Neeyalavira V, Tongsong T. Sonographic pattern recognition of endometriomas mimicking ovarian cancer. *Asian Pac J Cancer Prev* 2013; 14:5409–5413.
11. Buy JN, Ghossain MA, Mark AS, et al. Focal hyperdense areas in endometriomas: a characteristic finding on CT. *AJR Am J Roentgenol* 1992; 159:769–771.
12. Takeuchi M, Matsuzaki K, Uehara H, Nishitani H. Malignant transformation of pelvic endometriosis: MR imaging findings and pathologic correlation. *Radiographics* 2006; 26:407–417.
13. Siegelman ES, Oliver ER. MR imaging of endometriosis: ten imaging pearls. *Radiographics* 2012; 32:1675–1691.
14. McDermott S, Oei TN, Iyer VR, Lee SI. MR imaging of malignancies arising in endometriomas and extraovarian endometriosis. *Radiographics* 2012; 32:845–863.
15. Sampson JA. Endometrial carcinoma of the ovary, arising in endometrial tissue in that organ. *Arch Surg* 1925; 10:1–72.
16. Kobayashi H. Ovarian cancer in endometriosis: epidemiology, natural history, and clinical diagnosis. *Int J Clin Oncol* 2009; 14:378–382.
17. Nishimura K, Togashi K, Itoh K, et al. Endometrial cysts of the ovary: MR imaging. *Radiology* 1987; 162:315–318.
18. Togashi K, Nishimura K, Kimura I, et al. Endometrial cysts: diagnosis with MR imaging. *Radiology* 1991; 180:73–78.
19. Ghossain MA, Buy JN, Lignères C, et al. Epithelial tumors of the ovary: comparison of MR and CT findings. *Radiology* 1991; 181:863–870.